Acta Technica 62 (2017), No. 6B, 1309–1326

Motion tracking based on minimum sigma slope unscented particle reconstruction filtering

Fankun Meng[1], Yongfeng Ju[1], Jieru Yao[1]

Abstract. In order to improve tracking precision of mobile object, a mobile object tracking algorithm based on the minimum Sigma point slope particle reconstruction filtering is proposed in the thesis, which can better improve tracking precision of mobile object and reduce tracking energy consumption. The problem of uncertain target tracking under complex tracking environment was solved by taking advantages of divisive reconstruction tracker to fissure and reconstruct it so as to make parallel multi-trackers. Then, aiming at sub-tracker, taking advantages of the minimum Sigma point slope, particle filtering process was improved so as to improve calculation efficiency of unscented particle filtering algorithm. Simulation result verifies effectiveness of mentioned algorithm. The experimental result shows that compared with several selected positioning methods, mentioned tracking method can be used to obtain more optimized positioning effect at lower cost and can balance network load so as to improve service life of acquisition sensor network.

Key words. Unscented particle filtering, Particle reconstruction, Mobile target tracking, WSN, Target sensing.

1. Introduction

In the process of mobile target tracking, Wireless sensor network is a common solution with target sensing, data collection, and data processing performance [1]. Sensor is usually used for information receiving and sending in distributed and self-organized form. In the process of target tracking, numerous sensors are distributed in target position area for communication based on multi-hop wireless networks so as to complete target positioning. In the process of target tracking, WSNs should focus on solving problems in the following two aspects [2, 3]: (1) Positional precision of target; (2) energy consumption control of nodes so as to prolong network service life.

[1]School of Electronic and Control Engineering, Chang'an University, Xi'an City, Shannxi, 710064, China

In recent years, there are lots of research results in the aspect of target tracking algorithm, such as Literature [4] which uses enhanced and diversified particle filtering to realize organic integration of regional tracker, active tracker, and head tracker so as to obtain robust effect of pedestrian tracking. Integration of multi-trackers based on regional and central optimal data is proposed in Literature [5]; in addition, target state tracking shall be conducted by taking advantages of probability distribution function (PDF). Particle filtering target tracking is improved based on fixed color template in Literature [6]; in combination with random particle template, robust target tracker is realized. Inference integration of multi-trackers is realized by taking advantages of Kalman filtering so as to obtain optimal target position in Literature [7]. Particle filtering is used to realize synchronization of tracking process and detection process in Literature [8]; in addition, cascade form is used to obtain organic integration of three groups of trackers. Inconsistent strategies are used in Literature [9] so as to realize three-dimensional target positioning of WSN. Multi-trackers are used in literature [10] to track identical targets; tracking effect of trackers shall be optimized according to different environment or appearance. Above-mentioned methods can be used to solve recognition limitation of single tracker under complex environment; however, recognition method of multi-trackers will lead to greatly increase of computation complexity for the algorithm. Meanwhile, research shows that communication energy consumption in WSNs is higher than operation energy consumption of target sensing and CPU in Literature [11].

Therefore, in order to improve service life of WSNs, aiming at the problem of communication energy consumption which is not mentioned in above-mentioned literatures, divisive reconstruction tracker is firstly used to solve the problem of uncertain target tracking under complex tracking environment to fissure and reconstruct the tracker so as to make parallel tracker. Under the condition of reducing computation complexity, target can be subject to parallel tracking in different position and in different directions so as to reduce target losing probability, to avoid great energy consumption due to wrong search; in addition, UPF algorithm of the minimum Sigma point slope will be used to improve performance of sub-tracker.

2. UPF algorithm of the minimum Sigma point slope

The problem in traditional UPF is poor aggregation degree of Sigma, leading to heave computational burden of the algorithm. Therefore, the improved method is used to improve particle filtering process by taking advantages of the minimum Sigma so as to improve computational efficiency of UPF algorithm.

2.1. The minimum Sigma point set

$2n+1$ groups of Sigma points are required to be selected in the process of typical unscented transformation; however, n-dimensional simplex sphere has $n+1$ groups of sigma points, thus unscented transformation required for the minimum value sigma point can be accurate to second-order model. In consideration of variance and mean value of n-dimensional variable x, information about Sigma point is shown as follows:

in case χ_i^j is the state j of i-dimensional variable and vector; in case covariance and mean value of state vector separately are $P_{xx} = I$ and $\bar{x} = 0$.

In terms of one-dimensional space form, its Sigma point is

$$\chi_i^1 = \bar{x},\ s.t.\ i = 1; \chi_i^1 = \frac{-1}{\sqrt{2w_1}},\ s.t.\ i = 1\,.$$

$$\chi_i^1 = \frac{1}{\sqrt{2w_1}},\ s.t.\ i = 2\,. \tag{1}$$

Its weight coefficient is $\{w_i\}$, $i = 0, 1, 2$ and it conforms to:

$$\begin{cases} w_0 + w_1 + w_2 = 1, w_1 x_1^2 + w_2 x_2^2 = 1\,, \\ -w_1 x_1^2 + w_2 x_2^2 = 0, -w_1 x_1^3 + w_2 x_2^3 = 0\,. \end{cases} \tag{2}$$

Equation set (2) has solution under the condition of $w_1 = w_2$ and $x_1 = -x_2$ according to Equation (2), its result is:

$$w_i = w_0, i = 0; w_i = \frac{1 - w_0}{2}, i = 1, 2\,. \tag{3}$$

In terms of two-dimensional space form, No. of Sigma points increase to 4 groups; in case newly increased vector is $(0, x_3)$ and its corresponding weight is w_3, it can obtain:

$$\begin{cases} w_0 + w_1 + w_2 + w_3 = 1\,, \\ -w_1 x_3 + w_3 x_3 - w_2 x_3 = 0\,, \\ w_1 x_3^2 + w_2 x_3^2 + w_3 x_3^2 = 1\,, \\ -w_1 x_3^3 - w_2 x_3^3 + w_3 x_3^3 = 0\,. \end{cases} \tag{4}$$

Above-mentioned equation shall be solved so as to obtain $w_3 = 2w_1$ and $x_3 = 1/\sqrt{4w_1}$.

(3) $n+1$ dimension can be obtained according to recurrence of above-mentioned methods:

$$2w_1 + \sum_{i=3}^{n+1} w_i = 1 - w_0, w_{n+1} x_{n+1} - x_{n+1} W = 0,$$
$$W = \left(2w_1 + \sum_{i=3}^{n} w_i\right)\,.$$

$$w_{n+1} x_{n+1}^2 - x_{n+1}^2 W = 1, w_{n+1} x_{n+1}^3 - x_{n+1}^3 W = 0\,. \tag{5}$$

After solving above-mentioned equation, it can obtain:

$$w_i = \frac{1 - \mathrm{w}_0}{2}, s.t.\mathrm{i} = 1, w_i = w_1, s.t.\ i = 2,$$

$$w_i = 2^{i-2} w_1, i = 3, \cdots, n+1\,, \tag{6}$$

$$\begin{aligned}
&\chi_j^i = \left[\chi_0^{j-1}, 0\right]^T, i = 0; \chi_j^i = \left[0_{j-1} \frac{1}{\sqrt{2w_{j+1}}}\right]^T, i = j+1 \\
&\chi_j^i = \left[\chi_i^{j-1}, \frac{-1}{\sqrt{2w_{j+1}}}\right]^T, i = 1, \cdots, j
\end{aligned} \tag{7}$$

0_j is j-dimensional all-zero element vector and χ_j^i is the No. i element of vector with j dimension in above-mentioned equation. Sigma point shall be subject to sampling:

$$x_i = \bar{x} + \sqrt{P} \chi_i^n, i = 0, 1, \cdots, n+1\,. \tag{8}$$

2.2. Unscented variable-scale transformation

As entered covariance P_{xx} and mean value $\bar{x}$, variable x conducts sampling for Sigma point so as to obtain corresponding mean weight w_i^m and weigh covariance. If the problem of variable scale, then $w_i^m = w_i^c = w_i$; according to UT transformation principle, aggregation features of Sigma point can be improved by integrating α, β, κ so as to ensure half positive definiteness of matrix. In case x is n-dimensional random formal variable with covariance of P_{xx} and mean value of $\bar{x}$; in case y is the other random variable, $\bar{y}$ and P_{yy} can be calculated based on transmit transformation of nonlinear sample.

$$y = f\left[x\right]\,. \tag{9}$$

In order to obtain covariance and mean value of y, Taylor expansion shall be conducted at $\bar{x}$ point so as to obtain $f\left[\cdot\right]$. In case δx in $x = \delta x + \bar{x}$ is the random formal variable with zero of mean value and its covariance is P_{xx}

$$f[x] = f[\bar{x}] + \nabla f \delta x + \frac{1}{2} \nabla^2 f \delta x^2 + \frac{1}{3!} \nabla^3 f \delta x^3 + \cdots \tag{10}$$

Then, y shall be subject to covariance and expectation calculation:

$$\bar{y} = E[y] = f[\bar{x}] + \frac{1}{2} \nabla^2 f P_{xx} + \frac{1}{6} \nabla^3 f E[\delta x^3] + \cdots \tag{11}$$

$$\begin{aligned}
P_{yy} =& E[(y-\bar{y})(y-\bar{y})^T] \\
=& \nabla f P_{xx} (\nabla f)^T + \frac{1}{4} \nabla^2 f E[\delta x^3] (\nabla f)^T + \frac{1}{2} \nabla f E[\delta x^3] (\nabla^2 f)^T \\
&+ \frac{1}{2} \nabla^2 F \left(E\left[\delta x^4\right] + \frac{1}{3!} \nabla^3 f E\left[\delta x^4\right] (\nabla f)^T + \cdots \right)\,.
\end{aligned} \tag{12}$$

Variable-scale shall be used for Sigma point so as to improve dimension defects; these points are required to conform to the following equation:

$$z_i = \chi_0 + \alpha(\chi_i - \chi_0)\,. \tag{13}$$

Mean value of x shall be subject to non-linear transformation so as to obtain random variable $z = g\,[x, \bar{x}, \alpha, \mu]$

$$g[x, \bar{x}, \alpha, \mu] = \frac{f[\bar{x} + \alpha(x - \bar{x})] - f[\bar{x}]}{\mu} + f[\bar{x}]\,. \tag{14}$$

Where, α is positive scale, which shall be expanded at $\bar{x}$ point:

$$\begin{aligned} g[x, \bar{x}, \alpha, \mu] &= f[\bar{x}] + \nabla f \frac{\alpha}{\mu} \delta x \\ &+ \frac{1}{2} \nabla f \frac{\alpha^2}{\mu} \delta x^2 + \frac{1}{3!} \nabla^3 f \frac{\alpha^3}{\mu} \delta x^3 + \cdots \end{aligned} \tag{15}$$

Then, mean expectation value of z can be obtained:

$$\bar{z} = f[\bar{x}] + \frac{1}{2} \nabla^2 f \frac{\alpha^2}{\mu} P_{xx} + \frac{1}{6} \nabla^3 f \frac{\alpha^3}{\mu} E[\delta x^3] + \cdots \tag{16}$$

Unscented variable-scale transformation of random auxiliary variable shall be [12]:

$$\begin{cases} Z_i = \dfrac{f[\bar{x} + \alpha(\chi_i - \bar{x})] - f|\bar{x}]}{\alpha^2} + f\,[\bar{x}]\ , \\ \bar{z} = \displaystyle\sum_{i=0}^{p} W_i Z_i, P = \alpha^2 \sum_{i=0}^{p} W_i (Z_i - z)(Z_i - z)^T\,. \end{cases} \tag{17}$$

2.3. Algorithm steps

Local effect will be in lower dimension expansion of Sigma sampling point with increase of dimension. According to unscented variable-scale transformation specified in previous section, based on control parameter α and β, half positive definiteness of covariance matrix can be ensured. In addition, quantity of Sigma points can be reduced from $2n + 1$ to $n + 2$ so as to improve computational efficiency, which is shown in the following algorithm step 1 in detail:

Step1: Set $S_o = E[(x_0 - \hat{x}_0)(x_0 - \hat{x}_0)^T$ and $\hat{x}_0 = E[x_0]$

Step2: In case $k \geq 1$, $n+1$ groups of Sigma point χ_i and its corresponding weigh w_i can be obtained. Scale transformation shall be used; control parameters α and β shall be integrated; factor α shall be as proportional control parameter of Sigma point and $\alpha \in \left[10^{-4}, 1\right]$; β shall be integrated so as to obtain prior distribution information of x.

S2.1: Weight ω_{m0}, ω_{c0}, $0 \leq \omega_{m0} \leq 1$, and $0 \leq \omega_{c0} \leq 1$ shall be selected; then, the rest weight w_i shall be calculated according to equation (6); in addition, weight shall be revised according to proportion:

$$\omega_{m0} = \frac{\kappa}{n+\kappa}, \omega_{c0} = \frac{\kappa}{(n+\kappa)+(1-\alpha^2+\beta)}\,. \tag{18}$$

In combination with equation (6), according to unscented variable-scale result deduced from equation (17), the rest weight can be subject to the following scale transformation:

$$\omega_2 = \omega_1, \omega_i^m = \omega_i^c = \omega_i = \frac{2^{i-1}}{\alpha^2}, i = 3, 4, \cdots, n+1\,. \tag{19}$$

In the previous equation, $\kappa = \alpha^2 (n+\lambda) - n$ and w_i are weight of point i and conform to $\sum_{i=0}^{n+1} w_i = 1$

S2.2: One-dimensional point χ at the minimum slope shall be described:

$$\chi_0 = [0], \chi_1^1 = \left[\frac{-1}{\sqrt{2\omega_1}}\right], \chi_2^1 = \left[\frac{1}{\sqrt{2\omega_1}}\right]. \tag{20}$$

In the equation, χ_i^j is j-dimensional sampling point and 0_j is j-dimensional all-zero vector

S2.3: sequence shall be subject to n-dimensional expansion and $j = 2, \cdots, n$

$$\begin{aligned}
&\chi_i^j = \begin{bmatrix} \chi_0^{j-1} & 0 \end{bmatrix}^T, i = 0, \chi_i^j = \begin{bmatrix} \chi_i^j & -\frac{1}{\sqrt{2w_j}} \end{bmatrix}, i = 1, 2, \cdots, j \\
&\chi_i^j = \begin{bmatrix} 0_j & \frac{1}{\sqrt{2w_j}} \end{bmatrix}, i = j+1
\end{aligned} \tag{21}$$

$$\chi_i = (\chi_i^1, \chi_i^2, \cdots, \chi_i^n)^T\,. \tag{22}$$

Step 3: Sampling point shall be calculated:

$$\chi_k = \left[\hat{x}_k, \hat{x}_k + \sqrt{\alpha^2(n+\kappa)}\chi_1, \cdots, \hat{x}_k + \sqrt{\alpha^2(n+\kappa)}\chi_n\right]. \tag{23}$$

Step 4: Sigma point shall be spread:

$$\chi_{k|k-1} = f_k(\chi_{k-1}, k-1)\,. \tag{24}$$

Step 5: covariance and mean value of state $x_{k|k-1}$ shall be evaluated:

$$\begin{cases}
\hat{x}_{k|k-1} = \sum\limits_{i=0}^{N+1} \omega_i \chi_{i,k|k-1} \\
P_{k|k-1} = \sum\limits_{i=0}^{N+1} \omega_i (\chi_{i,k|k-1} - \hat{x}_{k|k-1}) \times (\chi_{i,k|k-1} - \hat{x}_{k|k-1})^T + P_\omega
\end{cases} \tag{25}$$

Step 6: prediction process is:

$$z_{k|k-1} = h_k(\chi_{k|k-1})\,. \tag{26}$$

Step 7: covariance and mean value are anticipated to be:

$$\begin{cases} \hat{z}_{k|k-1} = \sum_{i=0}^{N+1} \omega_i z_{i,k|k-1} \\ P_{z_k} = \alpha^2 \sum_{i=0}^{N+1} \omega_i (z_{i,k|k-1} - \hat{x}_{k|k-1}) \times (z_{i,k|k-1} - \hat{x}_{k|k-1})^T + P_v \end{cases} \tag{27}$$

$$P_{xz} = \sum_{i=0}^{N+1} \omega_i [\chi_{i,k|k-1} - \hat{x}_{k|k-1}][z_{i,k|k-1} - \hat{z}_{k|k-1}]^T \tag{28}$$

Step 8: covariance shall be subject to correction and filtering gain calculation:

$$\begin{cases} K_k = P_{xz} P_{z_k}^{-1}, \\ \hat{x}_k = \hat{x}_{k-1} + K_k (z_k - \hat{z}_{k|k-1}), \\ P_k = P_{k|k-1} - K_k P_{z_k} K_k^T. \end{cases} \tag{29}$$

Step 9: N particles shall be extracted:

$$x_k^{(i)} \sim N(x_k^{(i)}; x_k^{(i)}, P_k^{(i)}). \tag{30}$$

Step 10: particle weight shall be calculated:

$$\omega_k^{(i)} = p(z_k | x_k^{(i)}) \bar{\omega}_{k-1}^{(i)}, \omega_T = \sum_{i=1}^{N} \omega_k^{(i)}, \bar{\omega}_k^{(i)} = \frac{\omega_k^{(i)}}{\omega_T}. \tag{31}$$

Step 11: in case $N_{eff} < N_{th}$, $\bar{w}_k^{(i)} = 1/N$ is set; then, re-sampling process shall be implemented so as to obtain $\left[\left\{ x_k^{(i)}, w_k^{(i)} \right\}_{i=1}^{N} \right]$

Step 12: output result can be obtained:

$$\begin{cases} p(x_k | Z_{1:k}) = \sum_{i=1}^{N} \bar{\omega}_k^{(i)} \delta(x_k - x_k^{(i)}). \\ \hat{P}_k = \sum_{i=1}^{N} \bar{\omega}_k^{(i)} (\hat{x}_k - x_k^{(i)})(\hat{x}_k - x_k^{(i)})^T. \\ \hat{x}_k = E(x_k | Z_{1:k}) = \sum_{i=1}^{N} \bar{\omega}_k^{(i)} x_k^{(i)}. \end{cases} \tag{32}$$

α shall be used to conduct the minimum slope control for Sigma sampling:

$$d_i = \alpha \sqrt{\chi_i^j L L^T X_i^j}. \tag{33}$$

As the farther the sampling point is, the small the value is, thus the sampling point shall be subject to UT transformation:

$$y = f(x + \alpha(x - \bar{x}))\,. \tag{34}$$

α shall be used to adjust higher order term of error so as to improve estimated precision.

3. Parallel tracking for particle fission and reconstruction

3.1. Problem description

In terms of no covering or no interference, target tracking usually can obtain precision tracking result. However, target does not meet above-mentioned conditions in actual environment; interference will even exceed actual target weight, which is shown in Fig. 1.

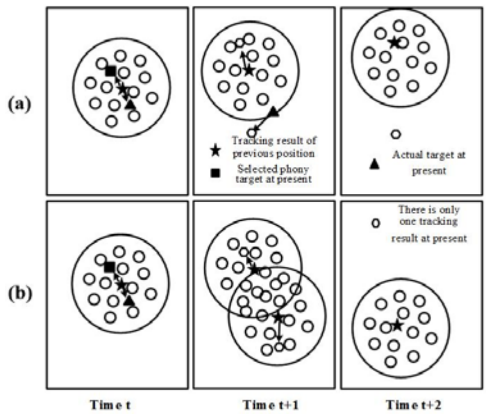

Fig. 1. The process of particle fission and reconstruction

Location data (five-pointed star) in previous iteration step shall be used as center of search area so as to obtain two groups of particles with larger weight in the area: there is certain failure probability in phony target algorithm, real target algorithm, and single target algorithm, leading to targeting losing, which is shown in Fig. 3a. Therefore, in terms of multi-target peak value, fission and reconstruction are designed to be used in fission and reconstruction process of particles so as to obtain multiple groups of particle tracker, which is shown as 3b and can effectively avoid wrong tracking of target.

3.2. Particle fission norm

Fission purpose is to reduce target losing probability and to avoid wrong fission problems at the same time. Therefore, the following fission norms are design:

Norm 1: Particle with the largest weight (Overlapped particle probability) is used to conduct state initialization for candidate set. When overlapping ratio of particle and all particle within candidate set are not higher than thresh value T_3, the particle shall be incorporated into candidate set. Both overlapping area and particle size shall be considered for used overlapping ratio, thus distance between two groups of particles can be more accurately represented with the norm form of:

$$R_{overlap} = \frac{A_1 \cap A_2}{A_1 \cup A_2}. \tag{35}$$

Norm 2: (Weight norm) according to norm 1, particles with higher overlapping ratio within the candidate set shall be eliminated; weigh threshold value shall be set as T_2, all particles shall be incorporated into weight and shall approach to 0 so as to form particle degeneracy after several times of iteration. In order to improve particle degeneracy, particle shall be subject to re-sampling process; particle noise will appear in the process; noisy particle has long distance with actual location; its likelihood value is low. Norm 2 can be used to eliminate noisy particles so as to improve positioning precision and to reduce calculation quantity.

Norm 3: (Target neighborhood) According to norm 1 and norm 2, all particles within candidate set can be marked with separate category; particles outside candidate set can be incorporated into relevant particle groups by taking advantages of overlapping ratio calculation. Then, reconstruction and filtering process of unscented particle with the minimum Sigma point slope shall be separately implemented within corresponding groups.

Information processing result of particle tracking process can be effectively improved so as to improve tracking effect of particle filtering algorithm through smooth implementation of three above-mentioned norms.

3.3. Reconstruction process

Purposes of reconstruction are: (1) to anticipate the most possible state of target; (2) to reduce quantity of trackers. In order to obtain trackers with the highest confidence coefficient, all confidence coefficients of all targets at all moments shall be accumulated; in case confidence coefficient of trackers are smaller than threshold value, these trackers shall be abandoned; in case their quantity is reduced to 1, the optimal target positioning prediction can be obtained. Confidence coefficient shall be defined to be [13∼14]:

$$Conf_{t+1}^{i} = \frac{Conf_t^i + f_t^i}{\sum\limits_{j=1}^{N} Conf_t^i + \sum\limits_{j=1}^{N} f_t^j}. \tag{36}$$

At the time of fission, mutual independence between tracker and target shall be ensured. In case there are more than 2 trackers which are used for tracking targets closely approaching predicted position; the two tracker shall be reconstructed and its optimal predicted mean value shall be selected to conduct initialization of new tracker so as to reduce quantity of tracker and to simplify calculation.

4. Unscented particle reconstruction filtering of the minimum slope at the point of Sigma

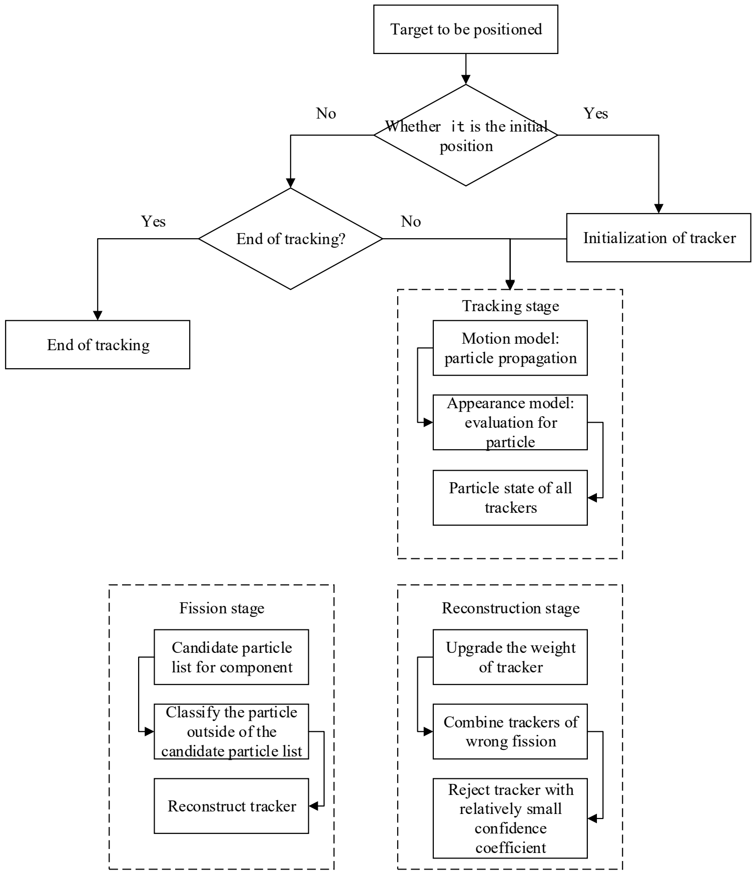

Fig. 2. Tracking algorithm flow

$$P\left(Z_t\left|X_t\right.\right)=e^{-\lambda d(H_r,H(X_t))}\,. \tag{37}$$

The target of the algorithm is based on the effective difference of overlapping state target by fission and reconstruction. For this, the following likelihood function is adopted[15]:

$$P\left(Z_t\left|X_t\right.\right)=e^{-\lambda d(H_r,H(X_t))}\,. \tag{38}$$

Including: λ is the preset constant; $H\left(X_t\right)$ is the distribution of candidate target; $d\left(H_r, H\left(X_t\right)\right)$ is the distribution distance. Fig. 2 shows the algorithm flow. See algorithm in detail.

Algorithm 2: Tracking algorithm flow

Input: sequence of target position, initial position of target, number of the particle.

Output: possible position of target in each step of iteration.

Initialization: initialize particle tracker and the initial value of confidence coefficient should be set as $Conf_0^1 = 1$, and the number of tracker is $N = 1$.

For $i = 1 : l$ do

/*tracking stage*/

- For target particle, target tracking and algorithm should be conducted based on N trackers

By adopting the steps in Section 2.3, the size and position information of all particles can be obtained. /*reconstruction stage*/

- Use form (37) to track the upgrading of weight of tracker.

- If the optimal overlapping ratio of target acquired by any two trackers is higher than T_o, then

reconstruct them.

Uniformization of weight of tracker and sequence them from largest to smallest;

- For $k = 1 \sim M$(M is the number of tracker)

- If $Conf_i^k \Big/ \left(Conf_i^{k+1} + Conf_i^k \right) > T$, then reject the tracker behind the mark number of $k + 1$

——End

/*Fission stage*/

- For $k = 1 \sim M$ (M is the number of tracker)

- Use the maximum weight of K tracker to initialize the candidate list S.

- Calculate the overlapping ratio of particle.

- For $n = 1 \sim p$(P is the corresponding particle number to tracker)

- If the overlapping ratio between particle n and candidate particle is smaller than T_1 and its weight is higher than T_2, then combine the particle to the candidate list S.

——End

- Classify the rest particle according to Criterion 3 and reject particle type that is smaller than Particle T_3.

- Reconstruct tracker according to the finally obtained candidate list.

- Uniformization of weight of reacker

——End

End

The above algorithm is integrated with fission and reconstruction process and has achieved the search of parallel target tracking. It has relatively strong anti-noise performance.

5. Experimental analysis

Experimental platform $SIDnct - SWANS$ of WSNs is adopted as the research object. Description of the experimental platform is shown in [16] of the Reference. Software downloading website is http://www.mccormick.northwestern.edu/eecs/.MAC-802.15.4Protocol is adopted in the platform and Face Routingprotocol is adopted for route protocol. Experiment parameter is shown in Table 1.

Table 1. Experimental parameters

Parameter	Numerical value
Number of nodes	1000
Transmission range	100m
Scan range	50m
Target speed	4,10,25(mph)
Node density	8,12,16,24
Noise of sensing $e \sim \left(0, \sigma^2\right)$	$\sigma = 1, 5, 10$
Particle number	5,10,20,50,100,200
Fault-tolerant threshold value	1,5,10,15,20
Sample rate	2s
Simulated time	2h

In addition, the selected parameters for the algorithm UPF of the minimum slope at the point of Sigma are as follows: $\alpha = 0.01$, $\beta = 2$, $\omega_0 = 0.5$. MSL and PFTL is selected for contrast positioning algorithm. The selected contrast method: (1) Contrast of the positioning error of three positioning method; (2) Influence of algorithm on variable values such as target mobile speed, node density and Particle number; (3) The service life of the network energy consumption of contrast algorithm and verification algorithm WSNs.

5.1. Influence of mobile speed

Fig. 3a shows the influence of object mobile speed on the accuracy of three positioning contrast method. From the Fig., as the target mobile speed is increased, error of positioning algorithm MSL tends to increase. Error of positioning algorithm PFTL remains unchanged because as the target mobile speed increase, the prediction interval of algorithm MSL will increase, leading to increase of error. Only node is used in positioning algorithm PFTL to link communication which has better relatively better stable positioning accuracy but poor accuracy value. The accuracy value of the algorithm in the thesis has increased by nearly 50% compared with that of positioning algorithm PFTL, nearly 35% compared with that of positioning algorithm MSL.

Fig. 3b shows the influence of tolerated error parameter on proposed positioning method. We can see that as the tolerated error parameter is increased, the accuracy of algorithm positioning is decreased. Relatively smaller tolerated error parameter value may be selected to maintain the algorithm positioning performance. But if the selected tolerated error parameter is too small, the calculating time of algorithm will be increased correspondingly and will influence real-time performance. Therefore, the selection should be reasonable according to the actual condition. Meanwhile, the faster the target moves, the less accurate of algorithm positioning will be.

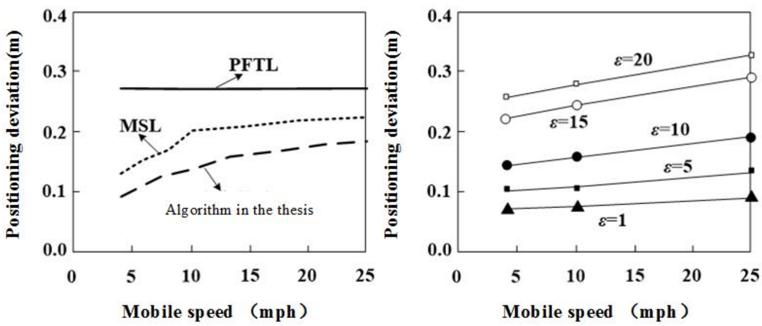

Fig. 3. Effect of mobile speed[(a) positioning error; (b) influence on the performance of the algorithm]

5.2. *Influence of node density*

Increase of node density (number/m^2) will cause frequent measurement. Although the positioning deviation can be lowered, the communication traffic will increase. Fig. 4 shows the result of the influence of node density on selected contrast positioning algorithm performance. We can see that the positioning accuracy of the algorithm in the thesis has increased by 34.3% and 23.6% respectively compared with that of positioning method PFTL and MSL. The reason is that the algorithm in the thesis can receive more anchor node data and the positioning accuracy is hence increased.

Fig. 4b shows the influence of node density parameter on proposed algorithm in the thesis. We can see that as the node density is increased, the algorithm positioning accuracy is increased. But if the selected node density parameter is too large, the calculating time of algorithm and deployment difficulty will be increased correspondingly and it will influence real-time performance. The selection should be reasonable according to actual condition.

5.3. *Influence of Particle number*

Only node is used in positioning algorithm PFTL to link communication which has relatively better stable accuracy so that the particle number has little influence on the performance of positioning algorithm PFTL but has large influence on the algorithm in the thesis and algorithm MSL. The details are shown in Fig. 5.

Fig. 5a shows the data of the influence of Particle number on the positioning method. When the particle number is small, the positioning accuracy of the algo-

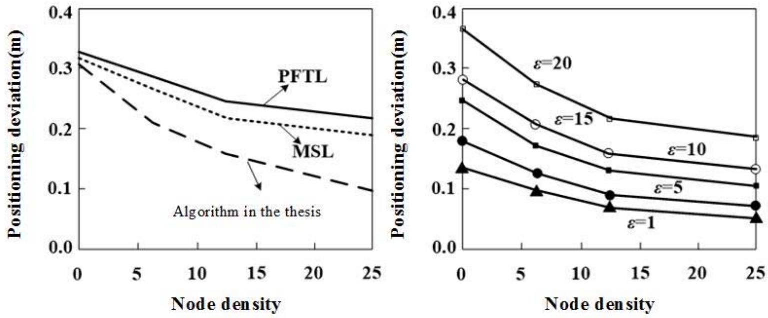

Fig. 4. Effect of node density [(a) positioning error; (b) influence on the performance of the algorithm]

rithm in the thesis and algorithm MSL is poor, even poorer than the positioning effect of algorithm PFTL. And as the particle number becomes larger, the positioning accuracy of the algorithm in the thesis and algorithm MSL is increased sharply, but the increasing effect of positioning accuracy due to the increase of particle number is gradually decreased. On the whole, the algorithm in the thesis is better than the positioning accuracy of algorithm MSL and PFTL. Fig. 5b shows the experiment on the influence of particle number on algorithm positioning performance. We can see that as the particle number is increased, the increasing effect of positioning accuracy of the algorithm in the thesis is gradually becoming gentle.

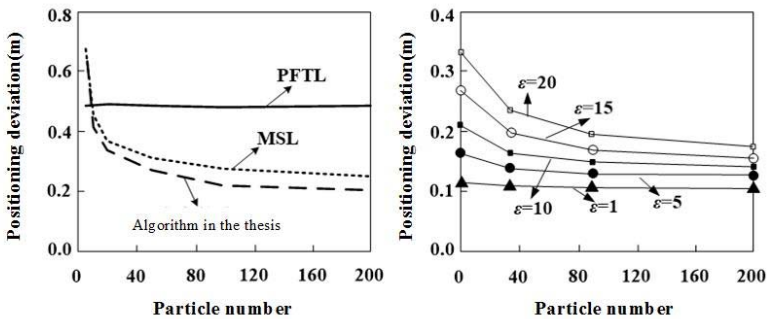

Fig. 5. Effect of particle number[(a) positioning error; (b) influence on the performance of the algorithm]

5.4. Network energy consumption analysis

Energy consumption analysis is conducted for the selected contrast positioning algorithm in the thesis. Node energy consumption is matched according to Standard Mica 2 Mote which is shown in Table 2. Contrast data of the experiment is shown in Fig.6.

Table 2. Parameter setting

State	Current (mA)	Energy (m J/ms)
Active sensing	10	0.03
Active CPU	8	0.024
Idle CPU	0.014	4.4*10-5
Radio transmission	26	0.082
Radio reception	11	0.04
Radio listening	3	0.008
Turn off the radio	0.6	0.0014

According to Fig. 6, we can know that the node energy consumption of the algorithm in the thesis is respectively decreased by 61.2% and 72.4% compared with that of positioning algorithm PFTL and MSL mainly in that tolerated error is adopted in the algorithm in the thesis to control node message routing to achieve the decrease of the burden of network energy consumption.

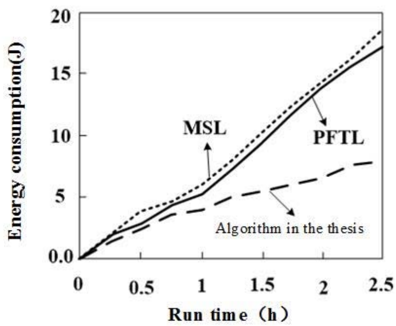

Fig. 6. Comparison of energy consumption

5.5. Contrast experiment on complex scenarios

The number of node adopted in the above experiment is 1000. To verify the target tracking performance in more complex scenarios, the range of variation of set node number is 2500-10000 and the value is obtained every 2500 nodes to verify the positioning deviation and energy consumption index of algorithm. The above two algorithms PFTL and MSL is still adopted in contrast algorithm. 10mps is selected as the mobile speed. Number 10 is selected as node density. Number 40 is selected as particle number. The position of $t = 2$s is selected as energy consumption. Other parameters are the same as the above. Experimental result is shown in Table 3.

Table 3. Contrast data in complex scenes

Algorithm	2500		5000		7500		10000	
	Positioning deviation	Energy consu-mption	Positioning deviation	Energy consu-mption	Positioning deviation	Energy consu-mption	Positioning deviation	Energy consu-mption
MSL	0.21m	18.3J	0.35 m	24.6 J	0.42 m	39.8 J	0.58 m	52.9 J
PFTL	0.27 m	17.9 J	0.39 m	23.7 J	0.41 m	37.4 J	0.56 m	50.1 J
Algorithm in the thesis	0.16 m	5.9 J	0.18 m	9.7 J	0.26 m	15.5 J	0.34 m	21.2 J

According to the data in Table 3, we can know that the positioning deviation value index of the algorithm adopted in the paper is the lowest compared with that of algorithm PFTL and MSL, but the overall difference is not that big, especially after the number of nodes is increased. Deployment Scenarios of node in the same node density will cause the increase of deployment area and the positioning deviation within an acceptable scope. As the energy consumption index, energy consumption of PFTL and MSL will substantially increase as the number of nodes is increased while the increase amplitude of energy consumption of the algorithm adopted in the thesis is far smaller than that of contrast algorithm, which shows the advantage of energy control of the minimum slope pattern at the point of Sigma.

6. Conclusion

A tracking algorithm for moving object of Particle reconstruction filtering based on the minimum slope at the point of Sigma is proposed. First, split-and-reconstruct tracker was used to solve the uncertain problem of the target tracking in complex tracking environment. When the computation complexity was decreased, multi-trackers formed by spilt and reconstruction can achieve parallel target tracking in multi-direction from different positions to reduce the losing probability of target; second, aiming at the aggregation degree difference of Sigma of unscented particle filtering (UPF), the big burden was calculated and particle filtering process was improved by the minimum slope at the point of Sigma and the tracker obtained from the sub-tracker to improve the computational efficiency of algorithm for unscented particle filtering; The framework proposed in the thesis has not taken consideration the heterogeneous of sensor and synchronization of node time. Therefore, for the organizational strategy for the network node under the network of heterogenization, how to achieve coordinate transformation of sensor, special allocation, data association etc. are key research issue in the future work.

Acknowledgement

National Natural Science Foundation of China (61473047); special fund for basic research business of Central University (2014G3322008).

References

[1] Liu Jingyuan, Liu Yun: (2015) *The optimization of location routing algorithm for location tolerance in WSN* [J]. Journal of Sichuan University (NATURAL SCIENCE EDITION), 52 (2): 338-342.

[2] Riccardo T, Francesco S, Claudio Pastrone, et al.: (2015) *Leveraging BIM Interoperability for UWB-Based WSN Planning*[J]. IEEE Sensors Journal, 15(10): 5988-5994.

[3] Luo Xu, Chai Li, Yang Jun: (2014) *Localization of near shore pollution sources in static water under wireless sensor networks* [J]. Journal of automation, 40 (5): 849-853.

[4] Malarvezhi P, Kumar R: (2015) *Particle Filter with Novel Resampling Algorithm: A Diversity Enhanced Particle Filter*[J]. Wireless Personal Communications, 84(4): 3171-3176.

[5] Zhou Bochao, Yang Shuo, Sun Tong, et al.: (2015) *A Novel Wireless Mobile Platform to Locate and Gather Data From Optical Fiber Sensors Integrated Into a WSN*[J]. IEEE Sensors Journal, 15(6): 3615-3624.

[6] Nadeem A, Mark R, Travis B, et al.: (2010) *Detection and Tracking Using Particle-Filter-Based Wireless Sensor Networks*[J]. IEEE Transactions on Mobile Computing, 9(9): 1332-1340.

[7] Alyamkin S A, Nezhevenko E S: (2014) *Comparative analysis of the efficiency of the Kalman filter and particle filter in solving the problem of object tracking in a seismic security system*[J]. Optoelectronics, Instrumentation and Data Processing, 50(1): 54-60.

[8] Movaghati S, Ardakani M: (2011) *Particle-Based Message Passing Algorithm for Inference Problems in Wireless Sensor Networks*[J]. IEEE Sensors Journal, 11(3): 745-752.

[9] Chen Yi, Jiang Zhaohui, Guo Chun: (2015) *An anti attack independent WSN security localization algorithm* [J]. Journal of sensing technology, 28 (11): 1702-1709.

[10] Zhang Ruimin, Chen Zhong, Li Xiaobin: (2015) *Bayesian WSN tracking and localization algorithm based on multi objective quantization variational filtering* [J]. Journal of Sichuan University (NATURAL SCIENCE EDITION), 52 (6): 1237-1244.

[11] Pablo B, Lutenberg A, Leonardo R V, et al.: (2014) *A Primer on Energy-Efficient Synchronization of WSN Nodes over Correlated Rayleigh Fading Channels*[J]. IEEE Wireless Communications Letters, 3(1): 38-43.

[12] Li Wenhua, Li Zheng: (2015) *Image matching algorithm based on dual scale SIFT descriptor and search region restriction* [J]. Journal of Sichuan University (NATURAL SCIENCE EDITION), 52 (2): 293-299.

[13] Shen Yin, Xiangping Zhu: (2015) *Intelligent Particle Filter and Its Application to Fault Detection of Nonlinear System*[J]. IEEE Transactions on Industrial Electronics, 62(6): 3852-3861.

[14] Jaehyun Yoo, Woojin Kim, Hyoun Jin Kim: (2015) *Distributed estimation using online semi-supervised particle filter for mobile sensor networks*[J]. IET Control Theory & Applications, 9(3): 418-427.

[15] Jung Min Pak, Choon Ki Ahn, Yuriy S Shmaliy, et al.: (2015) *Improving Reliability of Particle Filter-Based Localization in Wireless Sensor Networks via Hybrid Particle/FIR Filtering*[J]. IEEE Transactions on Industrial Informatics, 11(5): 1089-1098.

[16] Ghica O C, Trajcevski G, Scheuermann P, et al.: (2008) *SIDnet-SWANS: A platform for sensor networks applications*[C]. //Proceeding of the ACM Int'1 Conference on Embedded networks Sensor System, ACM, USA, pp.385-386.

Received May 7, 2017